RSC Advances

PAPER

View Article Online
View Journal | View Issue

Cite this: *RSC Adv.*, 2017, **7**, 47801

Higher-order glass-transition singularities in nano-confined states†

Changjiu Chen,[a] Kaikin Wong,[a] Rithin P. Krishnan,[a] Jan P. Embs[b] and Suresh M. Chathoth*[ac]

The dynamic processes of 2-biphenylmethanol (BPM) confined in carbon and silica pores with different sizes have been studied using the quasi-elastic neutron scattering (QENS) technique. A β-relaxation process following a logarithmic decay was found in both the nano-confined states. The peculiar features of the observed dynamic processes strongly agree with the predictions of the mode-coupling theory (MCT) for higher-order glass-transition singularities. The MCT critical temperature (T_c) of BPM, when confined in carbon and silica pores, was evaluated. The T_c was significantly low in the nano-confined states as compared to the bulk states. Furthermore, when comparing BPM confined in similar pore-sized carbon and silica materials, it was observed that the T_c was much lower for BPM confined in nano-porous silica materials. The generalized vibrational density-of-states of confined BPM indicated that the interactions of BPM with the silica pores is hydrophobic, whereas the interactions with the carbon surfaces is more hydrophilic. The different lowering of T_c for BPM depending on whether it is confined in carbon or silica materials is due to the different nature of the interactions between BPM and the confining surfaces of silica and carbon.

Received 16th August 2017
Accepted 15th September 2017

DOI: 10.1039/c7ra09049h

rsc.li/rsc-advances

Introduction

Understanding the behaviour of fluids in nano-confined states is of great importance in many scientific and technological fields. For instance, about 50–65% of the human body consists of water. However, water within the human body does not exist in its bulk form; instead, it is confined in crowded environments. Furthermore, interfacial water molecules control mineral dissolution, which is very important in earth science. Furthermore, water diffusion along the nanoscopic channels of polymer electrolyte membranes is central to the operation of hydrogen fuel cells. It is well-known that the properties of fluids confined in nano-scale dimensions differ from their corresponding bulk states.[1–4] For example, water crystallizes at 273 K in its bulk state. However, water confined in carbon nanotubes with a pore diameter of about 20 Å or less could be supercooled down to 190 K and upon further cooling, water transforms to an amorphous solid state.[5,6] This is due to the fact that the reduced dimensionality leads to enhanced surface effects.[7] In general, liquids confined in nano-pores can be supercooled well below their melting point, and the degree of supercooling has been found to be higher in hydrophobic pores than in hydrophilic pores.[8] This phenomenon allows us to study the properties of supercooled liquids, particularly the molecular relaxation processes occurring in supercooled glass-forming liquids.[9] The molecular relaxation processes occurring in bulk glass-forming liquids have been extensively investigated in the recent years.[10] In viscous glass-forming liquids, the molecules undergo two types of relaxation processes: (i) the fast β-relaxation, in which the molecules rattle inside a cage formed by neighbouring molecules and (ii) the slow α-relaxation, which consists of a long-range diffusion process.[11] In most liquids, the fast β-relaxation process follows a simple exponential decay.[12] However, recently, a logarithmic decay has been observed for the fast β-relaxation in 2-biphenylmethanol (BPM), phenyl salicylate (salol), *ortho*-terphenyl (OTP) and benzophenone (BZP) in their supercooled states by Optical-Kerr-Effect (OKE) experiments,[13–15] and in RNA and proteins by quasi-elastic neutron scattering (QENS).[16,17] However, the origin of such a complex relaxation process is not yet fully understood. Herein, we report the study by QENS of the effect of nano-scale confinement on a relaxation process characterized by a logarithmic decay.

Experimental methods

BPM ($C_{13}H_{12}O$, T_m = 320 K, T_g ~239 K) was obtained from Sigma-Aldrich. The materials used for confinement of

[a]*Department of Physics, City University of Hong Kong, Hong Kong, P. R. China. E-mail: smavilac@cityu.edu.hk*

[b]*Laboratory for Neutron Scattering and Imaging, Paul Scherrer Institute, 5232 Villigen PSI, Switzerland*

[c]*City University of Hong Kong Shenzhen Research Institute, Shenzhen, 518057, P. R. China*

† Electronic supplementary information (ESI) available. See DOI: 10.1039/c7ra09049h

BPM were nano-porous carbon with pore sizes of 39 ± 1 Å and 56 ± 1 Å, and nano-porous silica gel with pore sizes of 40 ± 1 Å and 60 ± 1 Å, which were purchased from ACS materials and Sigma-Aldrich, respectively. The Raman, FTIR and X-ray photoelectron spectra showed that there was no hydroxyl, carboxyl or silanol groups on the carbon or silica pore surfaces.[18] BPM was loaded onto the nano-porous carbon and silica materials *via* incipient wetness impregnation method, and the materials were 100% filled with BPM. The amount of BPM needed to completely fill the pores of 1 g of nanoporous carbon or silica powder was calculated, and this amount was dissolved in deuterated acetone (D-acetone). The carbon or silica powder was completely immersed in this liquid mixture and the system was kept open until D-acetone had evaporated. Subsequently, the BPM-loaded powder was heated at 80 °C overnight in a vacuum oven to completely evaporate residual D-acetone from the pores, leaving only BPM.

The QENS experiments were performed using a FOCUS time-of-flight neutron scattering spectrometer at the Paul Scherrer Institute, Switzerland.[19] We chose a neutron wavelength of 5.75 Å, which afforded an energy resolution of ~53 μeV (full-width at half-maximum). The accessible Q range at this wavelength was 0.4 $Å^{-1}$ to 1.8 $Å^{-1}$, and this experimental set-up covered the dynamical time window from 0.1 ps to ~15 ps. The QENS data were collected at 4 different temperatures: 300 K, 320 K, 340 K and 360 K. Since the incoherent neutron cross-section of hydrogen is the highest (80.26 barn), and the BPM molecule contains 12 hydrogen atoms, the scattering signals were mainly due to incoherent scattering processes. In addition, the samples were measured at 35 K in order to determine the instrumental resolution function. Empty sample containers were also measured at each temperature, and the scattering signal from a vanadium sample with a similar geometry to that of the test samples was applied to normalize the BPM scattering signals. The obtained raw data were converted into equidistant energy and momentum transfer steps using the Data Analysis and Visualization Environment (DAVE) software package.[20]

The QENS experiments for bulk BPM were performed using a MARS high-resolution indirect time-of-flight backscattering spectrometer (~13 μeV) at SINQ, Switzerland.[19] The scattered neutrons were filtered by a mica analyzer using the (0 0 6) reflection at a neutron wavelength of 6.61 Å. The accessible Q range was 0.4 $Å^{-1}$ to 1.7 $Å^{-1}$. The QENS data were collected at 5 different temperatures: 303 K, 313 K, 323 K, 333 K and 343 K. The bulk BPM sample was also measured at 10 K in order to determine the instrumental resolution function.

Results and discussion

The measured QENS intensity data were corrected for detector efficiency by normalizing it with the Vanadium data and subtracting the scattering contribution of empty sample containers and confining materials to obtain the incoherent dynamic structure factor, $S(Q,\omega)$ (Fig. 1). $S(Q,\omega)$ provides information on the dynamic processes within the sample and indicates the energy changes that occur during the scattering process as

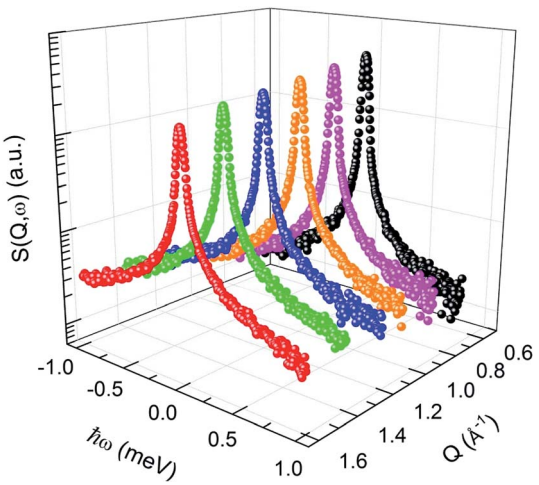

Fig. 1 Dynamic structure factor of BPM confined in silica pores (60 ± 1 Å) at 360 K in a semi-logarithmic representation.

a function of momentum transfer.[21] The generalized vibrational density-of-states, $G(\omega)$, of the confined BPM molecules were then calculated from the dynamic structure factor, $S(Q,\omega)$, measured at 35 K using the standard equation:

$$G(\omega) = \frac{S(Q,\omega)\omega}{Q^2[n(\omega,T)+1]} \quad (1)$$

where $n(\omega,T)$ is the Bose population factor. The resultant generalized vibrational density-of-states for the BPM molecules confined in carbon pores (39 ± 1 Å) and silica pores (40 ± 1 Å), shown in Fig. 2, were normalized with the weighted macroscopic scattering neutron cross-section of BPM on the neutron beam. The peak at around 5 meV is associated with translational vibrational motions (boson peak). This peak is more pronounced for BPM confined in 40 ± 1 Å silica pores as compared to that obtained for BPM confined in 39 ± 1 Å carbon pores. This indicates that the interaction of BPM with silica is more hydrophobic than the interaction of BPM with carbon. The self-intermediate scattering function, $\Phi(Q,t)$, was

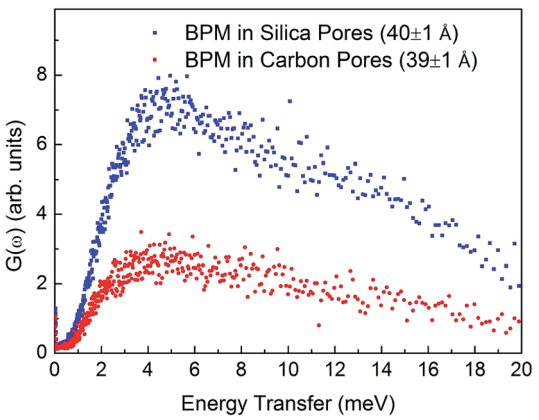

Fig. 2 Generalized vibrational density-of-states of BPM confined in carbon pores (39 ± 1 Å) and silica pores (40 ± 1 Å) measured at 35 K.

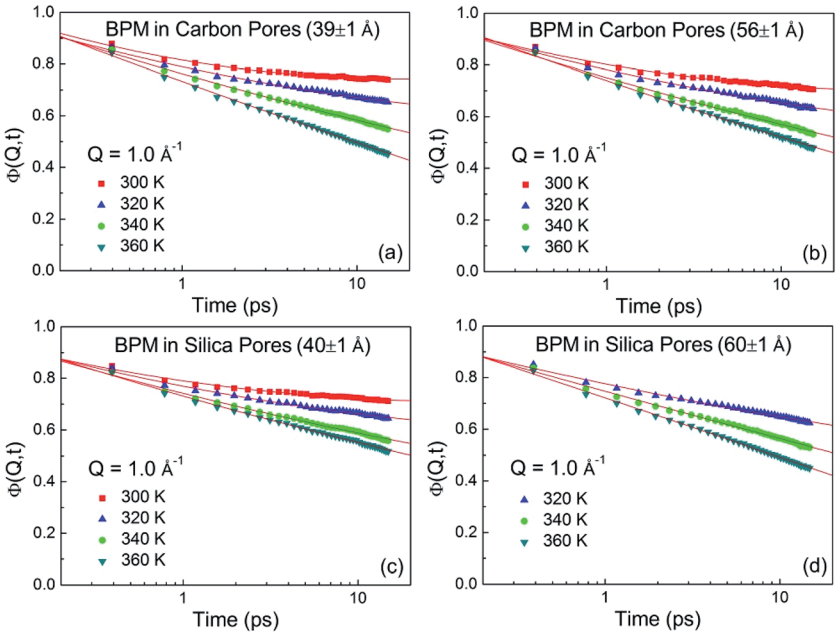

Fig. 3 Self-intermediate scattering functions of BPM confined in carbon pores (39 ± 1 Å) (a), carbon pores (56 ± 1 Å) (b), silica pores (40 ± 1 Å) (c) and silica pores (60 ± 1 Å) (d) at different temperatures. The error bars are within the symbols. The solid lines are fitting with eqn (2).

determined by Fourier transform of $S(Q,\omega)$ and convoluted with a resolution function. In a semi-logarithmic representation, the $\Phi(Q,t)$ decays linearly with time (Fig. 3). This is a clear indication that the relaxation process occurring in this time domain follows a logarithmic decay. The bulk BPM was found to exhibit a logarithmic decay relaxation process,[15] as shown in the ESI (Fig. 1S†). Our experiments showed that the logarithmic decay relaxation process persisted in the nano-confined states. This indicated that the complex β-relaxation process was not influenced by confinement in nano-scale dimensions with different surface interactions.

According to the mode-coupling theory (MCT), dynamic arrest occurs at a temperature well above the calorimetric glass-transition temperature, T_g. At the temperature where dynamic arrest occurs, also called the dynamic singularity point, the transport mechanism changes from molecular motions such as those in liquids to activated hopping processes such as those occurring in glass.[22] The MCT describes different types of singularities in the equations of motion for the density correlation functions. The equations can be classified as A_l, where $l = 2, 3,\ldots$ and $l = 2$ is the simplest singularity. It has been shown that in some systems with inter-particle potentials having hard-core repulsive and short-range square-well attractive components, dynamic arrest may occur *via* a different mechanism associated with higher order singularities such as A_3 or A_4. In these systems, the density correlation function for the fast β-relaxation process exhibits a logarithmic time dependence, and the following asymptotic formula derived from the MCT can be used for expressing the $\Phi(Q,t)$ corresponding to the β-relaxation process:[23–26]

$$\Phi(Q,t) \approx [f(Q,T) - H_1(Q,T)\ln(t/\tau_\beta(T)) + H_2(Q,T)\ln^2(t/\tau_\beta(T))] \quad (2)$$

where $f(Q,T)$ is the Debye–Waller factor, $f(Q,T) = \exp[-A(T)Q^2]$, and $\tau_\beta(T)$ is the characteristic β-relaxation time, which is Q independent. $H_1(Q,T)$ and $H_2(Q,T)$ represent the first- and second-order logarithmic decay parameters, respectively. The fitting-parameters, $f(Q,T)$, $H_1(Q,T)$, $H_2(Q,T)$ and $\tau_\beta(T)$, were obtained by fitting the curves in the measured time range. The Q dependence of $H_1(Q,T)$ parameter is shown in Fig. 4. The solid lines are the fitting lines as obtained by $H_1(Q,T) = B_1(T)Q$. The fitted $B_1(T)$ values are plotted as a function of the temperature in Fig. 5. The Q and temperature dependence plots of $H_2(Q,T)$ and $\tau_\beta(T)$ are provided in the ESI (Fig. 2S and 3S†). The plot corresponding to the temperature dependence of $B_1(T)$ (Fig. 5) was consistently extrapolated to obtain the MCT critical temperature, T_c. The T_c of bulk BPM was determined to be 282 ± 2 K, which is in good agreement with the value obtained in previous studies (290 ± 4 K).[14,15] This T_c value is approximately $1.2T_g$ (T_g ~239 K), which is universally observed. The T_c of confined BPM in nanoscale carbon pores with diameters of 39 ± 1 Å and 56 ± 1 Å was found to be 191 ± 2 K and 185 ± 2 K, respectively. Furthermore, the T_c of confined BPM in silica nanopores with diameters of 40 ± 1 Å and 60 ± 1 Å was 159 ± 2 K and 174 ± 2 K, respectively (see Fig. 5). For BPM confined in carbon nanopores, T_c was not substantially affected by pore size, despite the fact that the difference in pore diameter was nearly 20 Å. In contrast, for BPM confined in silica, T_c was found to be about 15 K lower in the 40 ± 1 Å pores as compared to that obtained for 60 ± 1 Å pores. Under confinement in a nanoscale environment, the properties of liquid molecules are mostly affected by the finite size of their environment and their interactions with the interfaces or the confining surfaces. The carbon nano-pores provide walls with strongly attractive interactions, while the silica nano-pores provide walls with relatively weak attractive interactions. Herein, the difference in the T_c values for BPM

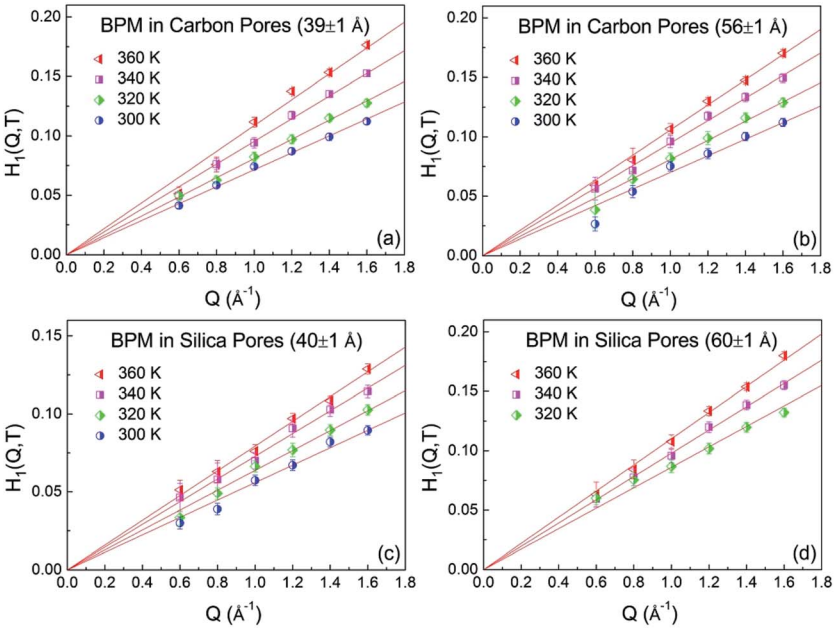

Fig. 4 Q dependence of fitting parameter $H_1(Q,T)$ for BPM confined in carbon pores (39 Å) (a), carbon pores (56 ± 1 Å) (b), silica pores (40 ± 1 Å) (c) and silica pores (60 ± 1 Å) (d) at different temperatures.

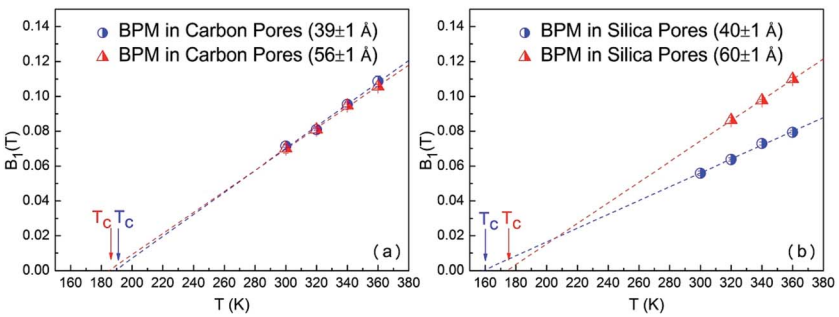

Fig. 5 Temperature dependence of $B_1(T)$ for BPM confined in carbon pores (39 ± 1 Å and 56 ± 1 Å) (a), and silica pores (40 ± 1 Å and 60 ± 1 Å) (b). The linear fitting lines were extrapolated to obtain the mode-coupling critical temperature, T_c.

when confined in silica or carbon nanoporous materials agrees with a universally observed behaviour: liquids can be supercooled to a much lower temperature in hydrophobic environments than in hydrophilic environments.

Conclusions

In summary, we have carried out QENS studies on 2-biphenylmethanol confined in carbon and silica nano-pores. A logarithmic decay for β-relaxation was observed in both nano-confined states within the time scale of the QENS data acquisition. The anomalous features of the dynamic processes are consistent with the mode-coupling theory predictions for higher-order glass transition singularities. The critical temperature values obtained from the analysis of the QENS data showed that T_c is significantly lower in the nano-confined states than in the bulk state. However, the decrease in T_c was found to be larger for BPM confined in silica nano-pores as compared to carbon nano-pores. The generalized vibrational density-of-states of confined BPM indicated that the interaction between BPM molecules and silica pores is hydrophobic, whereas the interaction with the carbon surfaces is more hydrophilic. The different nature of the interaction between BPM molecules and pore surfaces of carbon and silica results in a different value for the T_c depending on whether it is confined in carbon or silica.

Conflicts of interest

There are no conflicts to declare.

Acknowledgements

This research has been supported by Science, Technology and Innovation Committee of the Shenzhen Municipality, and the Basic Research Program under project no. JCYJ20140827151540605. All authors thank the Paul Scherrer

Institute (Switzerland) for providing beam time on the time-of-flight neutron scattering FOCUS instrument.

References

1 P. Huber, *J. Phys.: Condens. Matter*, 2015, **27**, 103102.
2 S.-H. Chen, F. Mallamace, C.-Y. Mou, M. Broccio, C. Corsaro, A. Faraone and L. Liu, *Proc. Natl. Acad. Sci. U. S. A.*, 2006, **103**, 12974–12978.
3 J. C. Saint Remi, A. Lauerer, C. Chmelik, I. Vandendael, H. Terryn, G. V. Baron, J. F. M. Denayer and J. Kärger, *Nat. Mater.*, 2016, **15**, 401–406.
4 N. C. Osti, T. N. Etampawala, U. M. Shrestha, D. Aryal, M. Tyagi, S. O. Diallo, E. Mamontov, C. J. Cornelius and D. Perahia, *J. Chem. Phys.*, 2016, **145**, 224901.
5 X. Q. Chu, A. I. Kolesnikov, A. P. Moravsky, V. Garcia-Sakai and S. H. Chen, *Phys. Rev. E: Stat., Nonlinear, Soft Matter Phys.*, 2007, **76**, 1–6.
6 S. M. Chathoth, E. Mamontov, A. I. Kolesnikov, Y. Gogotsi and D. J. Wesolowski, *EPL*, 2011, **95**, 56001.
7 V. Teboul and C. A. Simionesco, *J. Phys.: Condens. Matter*, 2002, **14**, 5699–5709.
8 R. Richert, *Annu. Rev. Phys. Chem.*, 2011, **62**, 65–84.
9 C. Alba-Simionesco, B. Coasne, G. Dosseh, G. Dudziak, K. E. Gubbins, R. Radhakrishnan and M. Sliwinska-Bartkowiak, *J. Phys.: Condens. Matter*, 2006, **18**, R15–R68.
10 C. A. Angell, K. L. Ngai, G. B. McKenna, P. F. McMillan and S. W. Martin, *J. Appl. Phys.*, 2000, **88**, 3113.
11 S. M. Chathoth, B. Damaschke, M. M. Koza and K. Samwer, *Phys. Rev. Lett.*, 2008, **101**, 37801.
12 A. Toelle, *Rep. Prog. Phys.*, 2001, **64**, 79.
13 G. Hinze, D. D. Brace, S. D. Gottke and M. D. Fayer, *Phys. Rev. Lett.*, 2000, **84**, 4783.
14 H. Cang, V. N. Novikov and M. D. Fayer, *Phys. Rev. Lett.*, 2003, **90**, 197401.
15 H. Cang, V. N. Novikov and M. D. Fayer, *J. Chem. Phys.*, 2003, **118**, 2800–2807.
16 X. Chu, M. Lagi, E. Mamontov, E. Fratini, P. Baglioni and S.-H. Chen, *Soft Matter*, 2010, **6**, 2623.
17 X. Chu, E. Mamontov, H. O'Neill and Q. Zhang, *J. Phys. Chem. Lett.*, 2013, **4**, 936–942.
18 P. A. Bazuła, A.-H. Lu, J.-J. Nitz and F. Schüth, *Microporous Mesoporous Mater.*, 2008, **108**, 266–275.
19 P. L. W. Tregenna-Piggott, F. Juranyi and P. Allenspach, *Neutron News*, 2008, **19**, 20–24.
20 R. T. Azuah, L. R. Kneller, Y. Qiu, P. L. W. Tregenna-Piggott, C. M. Brown, J. R. D. Copley and R. M. Dimeo, *J. Res. Natl. Inst. Stand. Technol.*, 2009, **114**, 341–358.
21 K. S. Singwi and A. Sjölander, *Phys. Rev.*, 1960, **119**, 863–871.
22 W. Götze and L. Sjögren, *Transp. Theory Stat. Phys.*, 1995, **24**, 801–853.
23 W. Götze and M. Sperl, *Phys. Rev. E: Stat., Nonlinear, Soft Matter Phys.*, 2002, **66**, 11405.
24 C. Chen, K. Wong, R. A. Mole, D. Yu and S. M. Chathoth, *Sci. Rep.*, 2016, **6**, 33374.
25 M. Lagi, P. Baglioni and S.-H. Chen, *Phys. Rev. Lett.*, 2009, **103**, 108102.
26 M. Sperl, *Phys. Rev. E: Stat., Nonlinear, Soft Matter Phys.*, 2003, **68**, 31405.